Bank erosion in regulated navigable rivers

Towards a process-based model of bank retreat

Duró, G. ; Crosato, A.; Uijttewaal, W.S.J.

Publication date
2020

Document Version
Final published version

Published in
River Flow 2020

Citation (APA)
Duró, G., Crosato, A., & Uijttewaal, W. S. J. (2020). Bank erosion in regulated navigable rivers: Towards a process-based model of bank retreat. In W. Uijttewaal, M. J. Franca, D. Valero, V. Chavarrias, C. Y. Arbos, R. Schielen, & A. Crosato (Eds.), *River Flow 2020: Proceedings of the 10th Conference on Fluvial Hydraulics* (1st ed., pp. 1254-1259). CRC Press / Balkema - Taylor & Francis Group. https://www.taylorfrancis.com/books/9781003110958

River Flow 2020 – Uijttewaal et al (eds)
© 2020 Taylor & Francis Group, London, ISBN 978-0-367-62773-7

Bank erosion in regulated navigable rivers: Towards a process-based model of bank retreat

G. Duró
Witteveen+Bos, The Netherlands

A. Crosato
Department of Water Engineering, IHE-Delft, The Netherlands

W.S.J. Uijttewaal
Department of Hydraulic Engineering, Delft University of Technology, The Netherlands

ABSTRACT: After the European Water Framework Directive, riverbanks in several countries had the protections removed to improve the water quality and the river ecosystem. Particularly, the Meuse River currently has several kilometres of freely eroding banks, which may have consequences for other river functions such as navigation and flood conveyance. The understanding, quantification and prediction of the morphological evolution of restored banks is thus relevant to manage the integrity of all river functions and improve future restoration practices. This work analyses the results of a recently developed model to estimate bank retreat in regulated waterways and compares them with measured profiles. The model essentially accounts for the major drivers of erosion, i.e., primary and secondary ship waves, considers homogenous cohesive banks, and computes erosion rates through a Partheniades-type of formulation. The results show a good qualitative and quantitative agreement with measurements. Erosion rates are yet not accurate with the current approach, for which future work will focus on improving the temporal representation through the inclusion of other factors and processes affecting erosion rates. These are, for instance, statistically representative time series of ship waves, currents during floods, and elements affecting erosion processes such as mass failures, slump-block dynamics and vegetation.

1 INTRODUCTION

The increasing pressure on river ecosystems (Best, 2018) demands for management practices that aim not only to preserve or optimize traditional functions, such as navigation and flood conveyance, but to promote habitat diversity for flora and fauna. Nevertheless, economic and ecological functions often present a conflict of interests (e.g., Boeters et al, 1997). The legislation in the European Union instructs to restore trained banks to improve the water quality and river habitats (WFD, 2000). Following this directive, the Meuse River in the Netherlands has had the bank protections removed along more than 40 kilometres during the last decade (see for instance, Figure 1).

The removal of bank protections reactivates erosion processes, which are particularly difficult to quantify and accurately predict in the case of navigable rivers (Bauer et al., 2002; Spruyt et al., 2012). A recently developed model has attempted to quantify the ultimate bank retreat induced by ship waves in regulated rivers (Duró et al., 2020). The goal of the present study is to analyze the predicted bank morphology by this model, compare it with measured profiles, and propose possible further developments to improve the accuracy to estimate bank retreat rates. The ultimate goal of this work is to allow for optimized management practices of multifunctional rivers.

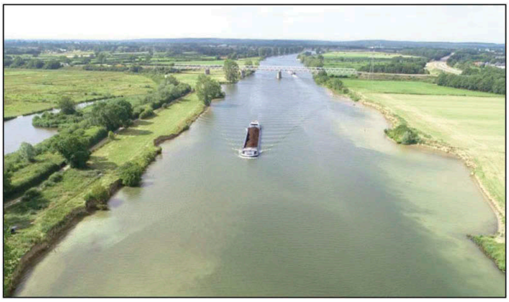

Figure 1. Re-naturalized banks in the Meuse River, the Netherlands.

2 METHODS

A case study in the Meuse River is used to analyze the capabilities of a model to predict bank retreat in regulated and navigable rivers. The morphological evolution of two measured banks with different erodibilities is analyzed and described. The results of the model applied to those cases are compared with the measured profiles. Next in this section, the study site, the bank characteristics, and the model are described.

The Meuse River has a pluvial regime with discharges ranging from 40 to 3000 m^3/s. The water levels are highly regulated through a sequence of weirs constructed during mid-20th century, for which 70% of the time the water stage remains at the minimum controlled level. This allows the river to function as a waterway throughout the year. At present day, approximately 30,000 vessels pass every year, generating primary and secondary waves that reach heights up to 0.45 m.

The two analysed bank types located at km 153.600 and 154.175 were both re-naturalized in 2010 through the complete removal of the riprap protections. The first bank is composed by sandy loam at the regulated water level, with $d50 = 0.11$ mm, and the second by silty loam at the same elevation, with $d50 = 0.02$ mm. The respective critical shear stress for entrainment are 6.4 and 12.6 Pa, estimated through the linear regression of Kimiaghalam et al. (2016) based on soil cohesion (Duró et al., 2019). The profile of these banks was measured in 2017 using UAV-SfM for the subaerial upper part during low flows (Duró et al., 2018), dGPS for the terrace, and Multibeam Echo Sounder for the submerged lower bank (courtesy of Rijkswaterstaat). In 2019, the terrace and subaerial part of the banks were measured with dGPS (see later Figure 2).

The applied erosion model computes the evolution of bank profiles through a Partheniades (1965) type of formulation (Equation 1):

$$\frac{dZ_b}{dt} = \varepsilon(\tau_b - \tau_c) \tag{1}$$

where Z_b is the bed elevation, ε is an erodibility coefficient, τ_b is bed shear stress induced by ship waves, and τ_c is the critical shear stress for entrainment of cohesive soils. τ_b are calculated considering primary and secondary waves. Primary waves are divided into drawdown, computed as a transverse current driven by the energy gradient during the maximum depression, and as a bore during upsurge, whose propagation and dissipation is modelled based on energy balance (Battjes and Jansen, 1978). The shoaling, refraction and dissipation of primary and secondary waves is calculated also based on energy balance. Run-up is considered using Bergsma et al. (2019) maximum height formula and Pujara et al. (2015) maximum shear stress distribution.

Mass failure of the upper bank and slump-block dynamics are not included in the model. The bank edge retreats by limiting the maximum topographic slope to 1:10. When the terrace

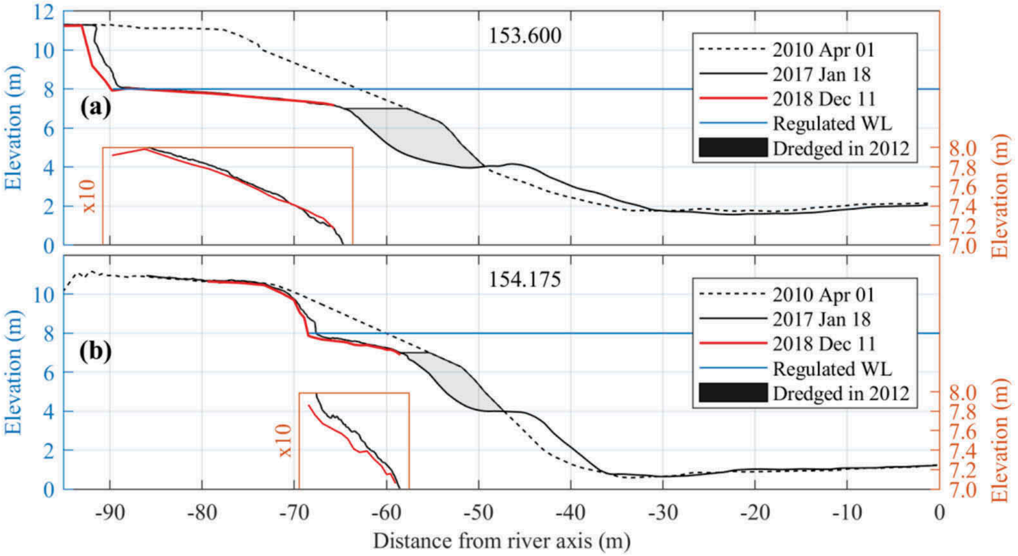

Figure 2. Bank profiles at km 153.600 (a) and 154.175 (b) showing bank erosion after 7 years and the terrace evolution over the following two years.

steepens beyond 1:10 at the bank toe due to erosion, the bank edge is moved backwards to match a slope of 1:10 starting from the bank toe. The model was calibrated with ε against measured profiles at other bank cross-sections in the Meuse River, arriving to a value of 0.01 m/s/Pa (Duró et al., 2020).

The necessary model inputs to estimate long-term or ultimate bank retreats are the critical shear stresses for entrainment of the dominant bank composition and the maximum wave heights of primary and secondary waves near the bank at a given site. For intermediate stages of bank retreat, lower wave heights are utilized. The model approach is based on the premise that the frequency of occurrence of waves determine different development stages, so that initial stages respond to most frequent waves and later stages are shaped by less frequent waves. A limitation of the current model version is that it is unknown in advance which wave height controls a given morphological stage of a bank. In the study location, the most frequent waves are small (≈0.10 m) while the highest waves (≈0.45 m) have the lowest probability of occurrence.

3 RESULTS AND INTERPRETATION

The measured bank profiles are shown in Figure 2, where 1st April 2010 profiles show the situations before the protections were removed. The most erodible bank presented a terrace of approximately 25 meters on 18th January 2017, which within the following two years had negligible erosion rates at the toe and relatively low erosion rates near the regulated level (Figure 2a). The second bank profile had a terrace of approximately 10 meters on 18th January 2017, which later experienced relatively low but measurable erosion rates at the terrace toe, and increasingly larger rates at higher elevations (Figure 2b). The upper-bank (scarp) erosion rates were higher for the silty-loam bank (a) than for the less erodible sandy-loam bank (b), despite the lower erosion rates at the terrace.

The short terrace remains at an early stage of development compared to the more erodible one, since it presented slower erosion rates. Between January 2017 and December 2018, waves still exerted high shear stresses over the terrace due to the short distance for their dissipation. On the other hand at km 153.600, the longer terrace allowed waves to gradually dissipate during the same period, since the precedingmorphological adaptation occurred faster. Despite the higher wave dissipation at km 153.600, the remaining energy reaching the upper-bank was still high enough to produce significant erosion rates, because here the material has a relatively high erodibility.

The model representation of the bank profiles on 18th January 2017 is shown in Figure 3. These correspond to primary wave heights of 0.25 m for km 153.600, and 0.20 m for km 154.175, and secondary waves of 0.45 m for both cases, but these exert significantly lower shear stresses than the primary waves. Both modelled profiles have a very good agreement with measured profiles over the first half of the terrace, defining accurate water depths at the toe. The bank retreat at the top panel is in good agreement with the measured profile, despite the overestimation of terrace erosion at the shallower area of the terrace. The bank at the lower panel (Figure 3b) overestimates bank retreat in approximately 30%, but the geometrical description of the bank matches reasonably well the measured profile.

The rates of bank erosion, however, significantly differ from those observed. Both profiles initially evolve at a fast rate, which substantially decrease close to the final stage. Figure 3a shows that the 2017 computed profile was reached after 4.4 years, representing 2/3 of the actual time (7 years). Figure 3b shows that 2017 modelled profile was reached after 4 months, far from observed rates.

4 DISCUSSION AND OUTLOOK

The current version of the ship-induced riverbank erosion model estimates the ultimate retreat for the case of regulated rivers. Intermediate development stages of the bank profile result from non-linear interactions with ship-induced waves. The model is able to reproduce reasonably well in qualitative and quantitative terms the bank geometry of measured bank profiles, by accounting for the essential driving processes. In this way, single wave heights are able to

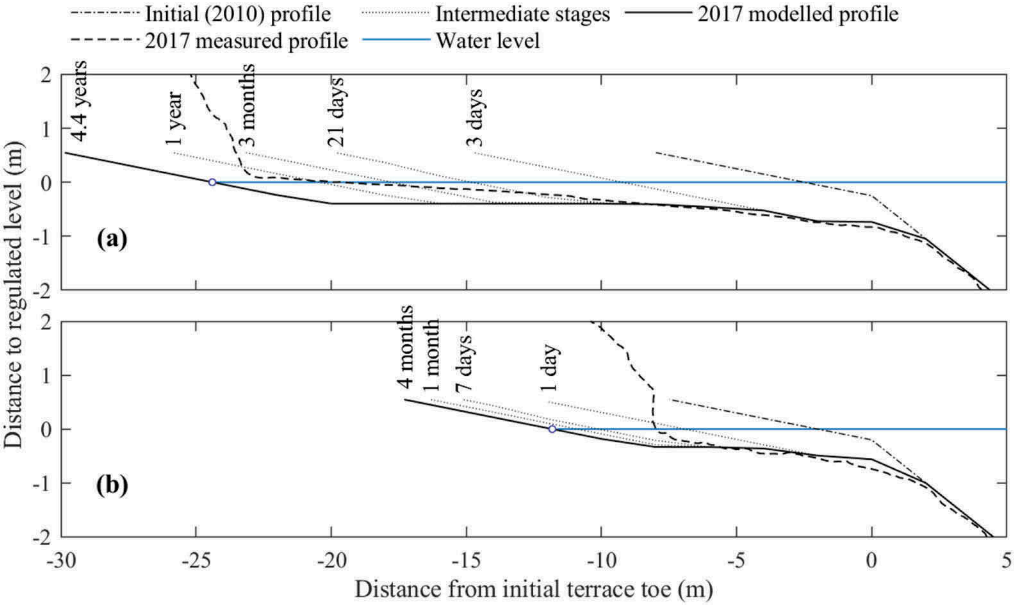

Figure 3. Model bank profiles corresponding to km 153.600 (a) and 154.175 (b) in 2017 (7 years after protection removal). Respective wave heights representing those stages are 0.25 and 0.20 m. Dotted lines indicate intermediate stages of the modelled bank before reaching the 2017 position, marked with continuous line. Terrace end is defined where the water level encounters the bank.

represent intermediate morphological stages (e.g., 2017 profile), despite the complexity of the system. Yet, the simulated temporal evolution differs from actual erosion rates due to missing processes and more realistic number and range of wave heights.

In order to increase the accuracy of predicted intermediate stages of bank retreat, future versions may incorporate the actual number and timing of different ship waves, covering the full range of wave heights, during intervals that represent intra-annual variations, e.g., monthly statistically representative time series. Chronological sequences would then account for non-linear morphological bank evolution that impact long-term morphologies (Southgate, 1995). Furthermore, the erodibility coefficient (ε) could be calibrated for different lithologies, overcoming the current model's limitation that produces, with single ε and wave frequency, great differences in erosion rates between different bank types.

The predictive accuracy of the terrace morphology could improve by including more processes affecting erosion rates. For instance, upper-bank erosion processes and the effects of flow currents during floods. Flow-induced shear stresses may be significant, especially during initial stages of bank development, and have feedbacks with ship waves that result in different erosion rates compared to individual factors. This addition implies the computation of mass failures and slump-block dynamics produced by both ship waves and currents, being challenging processes to represent and accurately estimate (Langendoen and Simon 2008; Parker et al., 2011). The lack of mass failures and slump-block dynamics is an important limitation of the current model. Their effects on bank retreat are absorbed by the calibration coeffient ε

Banks with extended terraces, as at km 153.600, sometimes present grown vegetation at the toe which affects erosion rates by attenuating wave loads and strengthening the soil. Such processes may eventually be incorporated as understanding and modelling predictive capacities improve (e.g., Bankhead et al., 2017).

5 CONCLUSIONS

The current process-based model represents reasonably well the terrace morphology shaped by ship waves in regulated rivers, which only accounts for ship-induced erosion over it. Still, predicted bank erosion rates are not sufficiently accurate for practical applications. The key promising steps to increase the precision of predicted temporal evolution are:

- Include a time series of the full range of wave heights and respective frequencies of occurrence, with representative monthly variations, for a more accurate calibration of the erodibility coefficient ε.
- Distinguish ε between different bank lithologies.

Additionally, more bank erosion processes could be added to the model, such as mass failures and slump-block dynamics, driven by flow currents and waves. These additions would add complexity to the model but could improve the morphological representation of the terrace morphology near the upper bank, and clearly the upper bank itself. After appropriate calibration, such model could also increase the predictive accuracy of bank erosion rates in navigable rivers.

REFERENCES

Bankhead, N. L., Thomas, R. E., and Simon, A. (2017) A combined field, laboratory and numerical study of the forces applied to, and the potential for removal of, bar top vegetation in a braided river. *Earth Surf. Process. Landforms*, *42*: 439–459.

Battjes, J. A., & Janssen, J. P. F. M. (1978) Energy loss and set-up due to breaking of random waves. In Coastal Engineering 1978 (pp. 569–587).

Bauer, B. O., Lorang, M. S., & Sherman, D. J. (2002). Estimating boat-wake-induced levee erosion using sediment suspension measurements. Journal of Waterway, Port, Coastal, and Ocean Engineering, 128(4),152–162.

Bergsma, E. W., Blenkinsopp, C. E., Martins, K., Almar, R., & de Almeida, L. P. M. (2019) Bore collapse and wave run-up on a sandy beach. Continental Shelf Research, 174, 132–139.

Best, J. (2018) Anthropogenic stresses on the world's big rivers. Nature Geoscience, 1.

Boeters, R. E. A. M., Havinga, H., Litjens, G., Verheij, H. J. (1997) Ten years of experience in combining ecology and navigation on Dutch waterways. 29th PIANC Congress.

Duró, G, Crosato, A, Kleinhans, M.G., Uijttewaal, W.S.J. (2018) Bank erosion processes measured with UAV-SfM along complex banklines of a straight mid-sized river reach. Earth Surface Dynamics 6: 933–953.

Duró, G., Crosato, A., Kleinhans, M.G., Winkels, T.G., Woolderink, H.A.G., & Uijttewaal, W.S.J. (2019) Distinct patterns of bank erosion in a navigable regulated river. Earth Surface Processes and Landforms.

Duró, G, Crosato, A, Kleinhans, M.G., Uijttewaal, W.S.J. (2020) Bank erosion processes in regulated navigable rivers. Submitted to *Journal of Geophysical Research: Earth Surface*.

Kimiaghalam N, Clark SP, Ahmari H. 2016. An experimental study on the effects of physical, mechanical, and electrochemical properties of natural cohesive soils on critical shear stress and erosion rate. International *Journal of Sediment Research 31*(1): 1–15.

Langendoen, E. J., & Simon, A. (2008) Modeling the evolution of incised streams. II: Streambank erosion. *Journal of hydraulic engineering*, 134(7),905–915.

Parker, G., Shimizu, Y., Wilkerson, G. V., Eke, E. C., Abad, J. D., Lauer, J. W., … & Voller, V. R. (2011) A new framework for modeling the migration of meandering rivers. *Earth Surface processes and landforms*, *36*(1), 70–86.

Partheniades, E. (1965) Erosion and deposition of cohesive soils. Journal of the Hydraulics Division, 91(1),105–139.

Pujara, N., Liu, P. L. F., & Yeh, H. (2015) The swash of solitary waves on a plane beach: flow evolution, bed shear stress and run-up. Journal of Fluid Mechanics, 779, 556–597.

Southgate, H. N. (1995) The effects of wave chronology on medium and long term coastal morphology. Coastal Engineering, 26(3-4), 251–270.

Spruyt, A., van der Sligte, R. A. M., van der Mark, C. F., Sieben, A., & Mosselman, E. (2012). *Development of a rapid assessment tool for river bank erosion*. Paper presented in River Flow 2012 (pp. 767–772). CRC Press.

WFD (2000) EU Water Framework Directive 2000/60/EC http://data.europa.eu/eli/dir/2000/60/oj, last access Dec. 2018).